Pergamon

PII: 80968-4328(97)00010-3

Micron Vol. 28, No. 3, pp. 249-265, 1997

0968-4328/97 $32.00+0.00

REVIEW PAPER

Automated Crystal Lattice Orientation Mapping Using a Computer-controlled SEM

ROBERT A. SCHWARZER

Institut für Metallkunde und Metallphysik der TU, Grosser Bruch 23, D-38678 Clausthal-Zellerfeld, Germany

(Received 7 October 1996; *accepted 3 January* 1997)

Abstract—A backscatter Kikuchi diffraction attachment to an SEM enables the convenient investigation of individual grain orientations on bulk surfaces. Their relation to microstructural features gives insight into many aspects of anisotropic materials properties. The formation of backscatter Kikuchi patterns and the experimental set-up for their acquisition are briefly outlined. The interactive and automated indexing of patterns and the fully Automated Crystal lattice Orientation Mapping (ACOM) with a computer-controlled SEM are presented in detail. Digital beam scan requires, as a consequence of the high tilt of the specimen with respect to the beam, current calculation of pattern centre and diffraction length (autocalibration) and dynamic focusing by the software. The automated measurement of lattice orientations takes less than half a second per image point on a Pentium Pro 200 MHz PC. Crystal lattice orientation maps (COM) are constructed by assigning to each grid point in the image a colour specific for the grain orientation, the misorientation or the grain boundary character. For a quantitative representation of the spatial distribution of microscale texture, an orientation-to-colour key is used by colour shading inverse pole figures, sections through Euler space or sections through Rodrigues orientation space. Texture components of interest can be highlighted by distinct colours in order to reveal textural inhomogeneities. Typical applications are given. © 1997 Elsevier Science Ltd

Key words: backscatter Kikuchi pattern, BKP, BKD, EBSD, crystal texture, ACOM, OIM, grain boundary, phase discrimination.

CONTENTS

I. INTRODUCTION

The study of preferred crystal lattice orientations ("crystallographic texture") with electron microscopes on a grain specific scale (Randle, 1992; Schwarzer, 1993a; Weiland, 1994) has become indispensable in materials science during recent years. For the measurement of individual grain orientations in particular, the "automated Kikuchi technique" with transmission electron microscopes (TEM) as well as with scanning electron microscopes (SEM) has been developed to a high standard. Electron-diffraction Kikuchi patterns in transmission from transparent thin foils, as well as in reflection from the bulk, were first described in 1928 (Kikuchi, 1928; Nishikawa and Kikuchi, 1928). Since then many examples of these types of Kikuchi pattern have been published (Boersch, 1937; von Laue, 1944; Wilman, 1948; Alam *et al,* 1954). Kikuchi patterns provide the microscopist with a convenient means of obtaining crystallographic information on a subgrain scale in the electron microscope. Kikuchi patterns, however, did not find a wide application in materials science until recently, mainly because of three experimental obstacles:

Abbreviations: ACOM *A*utomated *C*rystal lattice *O*rientation *M*apping/*M*easurement; COM *C*rystal lattice *O*rientation *M*ap; BKD *B*ackscatter *K*ikuchi Diffraction; BKP *B*ackscatter Kikuchi diffraction *P*attern; CBED *C*onvergent .*B*eam *E*lectron *D*iffraction; EBSD *E*lectron *B*ack*S*catter *D*iffraction (= BKD, usually SEM version using a video camera for recording the pattern); EBSP Electron *B*ack*S*catter *P*attern (= BKP); ECP *E*lectron *C*hannelling *P*attern; LEED *L*ow *E*nergy *E*lectron *D*iffraction; MBD *M*icro .*B*eam electron *D*iffraction; MODF *M*is*O*rientation *D*istribution *F*unction; ODF *O*rientation *D*istribution *F*unction; OIM® *O*rientation *I*mage *M*icroscopy (= ACOM); OIM® is a trade mark of TexSEM Lab. Inc., Heber City, Utah/USA; ORKID *O*rientation from *K*ikuchi *D*iffraction; RHEED *R*eflection *H*igh *E*nergy *E*lectron *D*iffraction; SAD *S*elected *A*rea electron *D*iffraction; SEM *S*canning *E*lectron *M*icroscope / *M*icroscopy; STEM *S*canning *T*ransmission *E*lectron *M*icroscope / *M*icroscopy; Σ value reciprocal value of the fraction of the coincident lattice sites of two superimposed crystal lattices; TEM *T*ransmission *E*lectron *M*icroscope / *M*icroscopy; TKP *T*ransmission *K*ikuchi diffraction *P*attern.

they depend on a finely focused primary beam for their generation from technical materials, which are often characterised by a small grain size and imperfect crystal structure. They require a clean vacuum in the specimen chamber of the microscope in order to suppress the growth of contamination patches of hydrocarbons polymerised under the primary-beam spot. Finally, their interpretation is more laborious than spot patterns in the TEM or X-ray diffraction patterns. For the study of crystallographic texture in particular, an immense number of individual grain orientations has to be known, which makes a computer mandatory for the interpretation of diffraction patterns.

In the late sixties, video systems became gradually common for recording faint images and diffraction patterns in the TEM. The attachment of a video camera to the SEM (Venables and Harland, 1973) enabled the live display of backscatter Kikuchi patterns from bulk surfaces. However, image quality was poor, the sensitivity of the cameras low and the required probe currents rather high, such that this technique could not yet compare with SAD channelling patterns when used for example for grain boundary characterisation (Watanabe, 1983). A breakthrough in the application of Kikuchi patterns to bulk samples in materials science was marked by the development of a system for recording backscatter Kikuchi patterns on an SEM by using a highly sensitive video camera and a computer-assisted indexing method (Dingley, 1984). At that time, however, the operator had still to identify three low-index poles in the pattern by visual inspection ([112], [111] and [114]). Cubic crystal symmetry was supported.

The interactive on-line interpretation of Kikuchi and channelling patterns from obliquely oriented grains was first realised for the TEM with the "ORKID" program (Schwarzer and Weiland, 1984). The acronym ORKID stands for "crystal lattice ORientation from Kikuchi Diffraction". The user had to enter the positions of at least three deliberately selected bands. He had to shift the live diffraction pattern across the viewing screen, a procedure which corresponds to the positioning of the mouse cursor on the monitor screen in present systems. The indexing of the bands was performed automatically by considering the Bragg equation, i.e. the interplanar spacings d_{hkl}, and the interplanar angles of the most prominent lattice planes, as given by the structure factor. The crystal lattice orientation was then computed and expressed by (*hkl*)[*uvw*] notation for two sample reference directions. A simulated Kikuchi pattern for this orientation was displayed on the computer monitor, to allow a check of correctness. Cubic, hexagonal and tetragonal crystal symmetry were supported.

A similar interactive procedure had been developed for backscatter Kikuchi patterns (Schmidt and Olesen, 1989; Schmidt *et al.,* 1991). Since then, the fully automated orientation measurement has been realised using the Burns or Hough algorithms for locating band positions in backscatter Kikuchi patterns (Wright *et al,* 1991; Juul Jensen and Schmidt, 1991) and in transmission Kikuchi patterns (Zaefferer and Schwarzer, 1994a; Krieger Lassen, 1995). The culminating result of this exertion is a new technique of materials characterisation, the Orientation Imaging Microscopy (Adams *et al,* 1993), or the Automated Crystal lattice Orientation Mapping (ACOM) as described here.

About 45 years after the first description of backscatter Kikuchi patterns in the literature, the terms "EBSP" or "EBSD" were introduced as acronyms for "Electron BackScattering Pattern" or "Electron BackScattering Diffraction" (Venables and Harland, 1973). The new terms for the same kind of electron diffraction, however, could obscure the close relation between backscatter and transmission Kikuchi patterns (BKP and TKP) and could be misleading. Backscattered electron diffraction, as the alternative to transmission electron diffraction, comprises, besides backscatter Kikuchi diffraction (BKD), several other widely used diffraction techniques such as low energy electron diffraction (EEED) and reflection high energy electron diffraction (RHEED, in particular backscattered electron spot and texture patterns) with a stationary primary beam as well as channelling patterns in the SEM with a rocking primary beam.

II. THE GENERATION OF BACKSCATTER KIKUCHI PATTERNS

The basic principles of formation of transmission and backscatter Kikuchi patterns are the same. Since only the geometric features, i.e. the positions of Kikuchi bands and lines in a pattern, rather than the diffracted intensities are required for indexing and orientation measurement, the kinematic model as introduced by Kikuchi (1928) is adequate here. The finer details in a pattern such as the distribution of band intensities or curved lines (Kikuchi envelopes) are well understood from dynamic theory simulations (von Laue, 1944; Hashimoto *et al,* 1962; Reimer *et al,* 1986).

In the SEM, Kikuchi patterns are formed if some portion of the stationary primary electron beam is scattered inelastically, or at least incoherently, through large angles when entering a crystalline specimen (S in Fig. 1). The beam convergence has virtually no effect on the formation of Kikuchi patterns since inelastic scattering spreads the primary beam into all directions, and the term "convergent beam diffraction" (CBED) is not appropriate for this type of electron diffraction. A large angle of beam convergence, however, is inevitable for producing a small and intense primary beam spot on the sample. Hence the term "microbeam electron diffraction" (MBD) is appropriate for this technique if a high spatial resolution is intended. The crystal lattice planes in the interaction volume beneath the surface are thus exposed to a shower of electrons from all directions. Those electrons which impinge upon lattice planes *hkl* along a cone at an opening angle of $(90° - \theta)$ may be mirrored according to Bragg's law

$$2\, d_{hkl} \sin\theta = n\lambda \qquad (1)$$

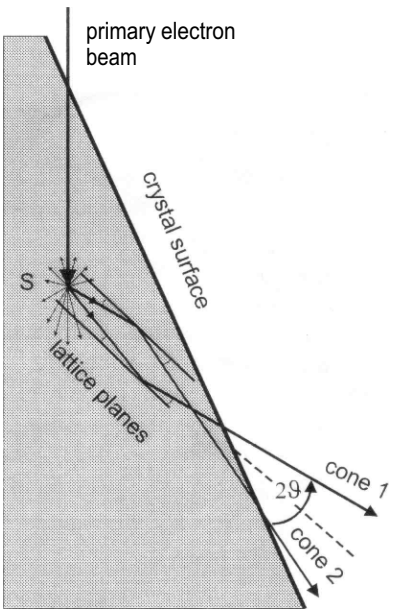

Fig. 1. Formation of a backscatter Kikuchi band (schematic).

where d_{hkl} is the interplanar spacing, θ the Bragg angle, n is an integer (the order of reflection) and λ the electron wavelength. The rest of the inelastically scattered electrons form a continuous background. Inelastic scattering is more pronounced in the forward direction with the maximum of intensity falling approximately into the direction of optical reflection (Alam *et al.,* 1954; Niedrig, 1978). Hence the diffraction cones (also named Kossel cones) usually differ in intensity. If mirroring takes place from a direction closer to the primary beam to a direction further away, there is more intensity in the outgoing beam on that cone than in the background. A bright excess Kikuchi line appears on a phosphor screen close to the crystal. If mirroring results in a deflection to a direction closer to the primary beam, the opposite is true and a dark defect Kikuchi line is visible. The angular distance between a pair of Kossel cones is twice Bragg's angle; the lattice plane, imaginarily stretched out (dashed line in Fig. 1), seems to intersect with the phosphor screen in a trace line midway between both Kossel cones.

Some essential features follow from this simplified model and explain why Kikuchi patterns are well suited for the accurate determination of crystal lattice orientations. First, the loss of energy by an inelastic scattering event is small compared to the beam energy. Hence the spread in wavelength of diffracted electrons is small, and Kikuchi lines are extremely sharp. Secondly, the Kossel cones are rigidly fixed in orientation to their lattice planes. Hence a Kikuchi pattern exactly follows any rotary movement of the crystal lattice. Third, the centre line between a pair of Kossel cones corresponds to the intersection line of the lattice plane made with the phosphor screen. Hence the angles between centre lines correspond to the interplanar crystallographic angles provided that allowance is made for distortion by projecting the pattern on a plane screen. Fourth, the Bragg angles are rather small for energetic electrons (≈ 0.5°). Hence the sections of a pair of Kossel cones with the flat phosphor screen form a pair of virtually parallel straight Kikuchi lines, a feature which makes measurement and calculations quite easy. Fifth, the pattern geometry as a whole is rather simple. It corresponds to a gnomonic projection of the lattice planes on the flat phosphor screen with the target point of the primary beam spot in the crystal acting as the centre of projection.

In contrast to transmission Kikuchi patterns from thin samples, Kikuchi lines are often missing in backscattered electron diffraction, whilst the regions between the expected line pairs exhibit an excess of intensity. These straight bands are named Kikuchi bands. They are characterised by the same crystallographic features as the line pairs above: A band is 2θ wide, and the centre line corresponds to the section line of the related lattice planes. A sharp drop of intensity is found at the Bragg angles, i.e. at the positions of the Kikuchi lines. It is quite complicated to describe the formation of Kikuchi bands quantitatively by using the dynamic theory of electron diffraction, and the reader is referred to Reimer *et al.,* (1986). The basic concept is that an electron wave is channelled deep into the crystal if it propagates at an angle θ along a low index lattice plane, while it is blocked for angles $<\theta$. The result is an enhanced interaction of the primary beam in a shallow region beneath the surface (and an increased backscattered electron intensity) for directions within $\pm\ \theta$ of low-index lattice planes. Therefore bright bands are formed in backscatter Kikuchi and backscatter channelling patterns. The Bragg reflection positions at the band edges are the lines where the intensity is equal to the background intensity in the region considered. In some cases, however, a contrast reversal from excess to defect band intensity is reported (Alam *et al,* 1954; Reimer, 1979) at larger angles of incidence for regions in the pattern close to the shadow edge from the specimen surface.

The diffracting volume of the specimen has to be virtually a perfect crystal, otherwise the individual Kikuchi patterns from bent regions or mosaic subcrystals within the illuminated field are superimposed and a diffuse integral pattern is obtained which is easily submerged by the background. With samples made from real materials, the condition for a perfect crystal may be fulfilled by focusing the primary beam to a small spot on the area under study (MBD), such that the beam passes through a crystal volume of low local dislocation density. The demand for a perfect crystal volume is alleviated because dislocations often arrange themselves in networks. If necessary, a gentle anneal is possible and does not change the crystal lattice orientation.

Backscatter Kikuchi patterns in the SEM often appear less crisp than transmission Kikuchi patterns recorded on film in the TEM, and may be so diffuse that Kikuchi lines are hardly visible. As has been demonstrated by examples of clear backscatter Kikuchi patterns in the literature (Heise, 1952; von Grote, 1968/69; Gaukler and Schwarzer, 1971; Ino, 1977; Reimer, 1979), this is not due to some peculiarities of backscattered electron diffraction. The reasons for blurred backscatter Kikuchi

patterns in the SEM include an inadequately large diffracting volume which contains an excessive density of dislocations or subgrains. Secondly, photographic film is still superior in image quality to usual video cameras (Reimer and Grun, 1986). Third, a poor design of the low-light level video camera system in some SEM set-ups may give rise to noise and loss in high-frequency signal which drastically deteriorates the image. It is obvious that a first-grade macro objective lens is indispensable with a lens-coupled video camera. A remarkable improvement in image quality of backscatter Kikuchi patterns is obtained by integrating the diffraction pattern on a cooled CCD camera chip and transmitting the image to the computer in one step, either as a single frame at standard video frequency (Schwarzer, 1989) or—as a much superior approach—in broad-band slow-scan mode (Michael and Goehner, 1993). In standard set-ups, however, the diffraction pattern is passed on to the computer, digitised and averaged frame-by-frame at video frequency, resulting in a reduced signal-to-noise level.

Electron channelling patterns (ECP) are geometrically very similar to Kikuchi patterns. They are produced with the electron beam pivoting above a fixed point on the specimen (i.e. the selected area) rather than scanning in a raster across the specimen as is the case in the ordinary imaging mode of an SEM. Backscattered electrons, secondary electrons, the probe current or—from thin specimens—transmitted electrons can be used as the source of signal. The diffraction image is formed on the SEM display screen by mapping the measured intensity point-by-point against angles of incidence on a Cartesian coordinate frame. The angular range of a channelling pattern is limited by the rocking angle of the primary beam (typically 5-10°). A channelling pattern can be detected only if the divergence of the primary beam is in the range 10^{-3} to 10^{-4} rad; i.e. smaller than the Kikuchi line width and much less than the Bragg angle, otherwise the pattern becomes too diffuse. The direction of incidence continuously varies during the beam scan. The penetration depth of the primary beam strongly depends on its crystallographic direction. A sharp drop is encountered every time the beam approaches close to a low index lattice plane and passes across the Bragg angle, resulting in an increase in backscattered intensity, so the crystallography of the grain is reflected in the channelling pattern. It consists of a series of bands whose widths and the angles between them are related to interplanar spacings and angles in the same way as with Kikuchi patterns. Hence the same procedures for on-line indexing can be used (Weiland and Schwarzer, 1985; Schwarzer and Zaefferer, 1994).

Channelling patterns have some advantages over backscatter Kikuchi patterns from bulk samples: The specimen stands normal to the optic axis of the microscope column, so the image of the microstructure is not distorted. The sample can be placed at a low working distance close to a solid state detector which ensures an excellent contrast in the microstructure image as well as in the diffraction pattern. The pivot point can be slightly widened to form a raster frame on the sample. If a grain boundary passes through this field, the channelling patterns of both abutting grains are displayed simultaneously side by side in the diffraction 'image' of the scanned field. Hence a very accurate determination of the misorientation across the grain boundary is enabled. Serial acquisition of the channelling pattern can be carried out at a slow scan rate with a very low primary beam current and yet low noise, such that delicate samples may be studied. Channelling patterns are provided as a standard option with some SEMs. However, since spatial resolution is more than one or two orders of magnitude poorer (due to the large objective lens aberration at large rocking angles of the primary beam) and a more stringent specimen preparation is required, channelling patterns have been superseded during the last decade by backscatter Kikuchi patterns for most applications in materials science.

III. EXPERIMENTAL ARRANGEMENTS FOR THE ACQUISITION OF BACKSCATTER KIKUCHI PATTERNS

Backscattered electron diffraction, as an add-on technique for measurement of individual grain orientation with an analytical SEM, has become indispensable in materials science. Several experimental arrangements have been designed for the acquisition of backscatter Kikuchi patterns. Dedicated electron-diffraction equipment had been used earlier to study the principles of backscattered electron diffraction or for applications in surface science. An add-on BKD facility to the SEM (Venables and Bin-Jaya, 1977) offers the unique advantage of enabling convenient study of the crystallography and the acquisition of an SEM image of the microstructure of a very localised and well-defined place in the specimen surface. To collect maximum intensity in the diffraction pattern by capturing the most intense fraction of inelastically scattered electrons, the specimen surface is steeply tilted at an angle of typically 20-30° from grazing incidence. A smaller angle down to grazing incidence might further improve intensity and is indispensable in the study of surface effects (RHEED), but at the expense of spatial resolution. Disadvantages of the high specimen tilt in backscatter Kikuchi diffraction are the foreshortened beam spot on the sample as well as the foreshortened images. For the acquisition of backscatter Kikuchi patterns either a photographic plate or a phosphor screen has been placed parallel to the incident beam, right in front of the tilted sample, or beneath the specimen and normal to the primary beam. The intensity of backscatter Kikuchi patterns is rather low and contrast is in the range of 5% or less, so extremely sensitive cameras and contrast enhancement facilities are required.

Our set-up for recording backscatter Kikuchi patterns on an SEM is shown in Fig. 2 (Schwarzer, 1994a). The system is attached to the rear port of the specimen chamber of a JEOL JSM 6400 SEM. The specimen is

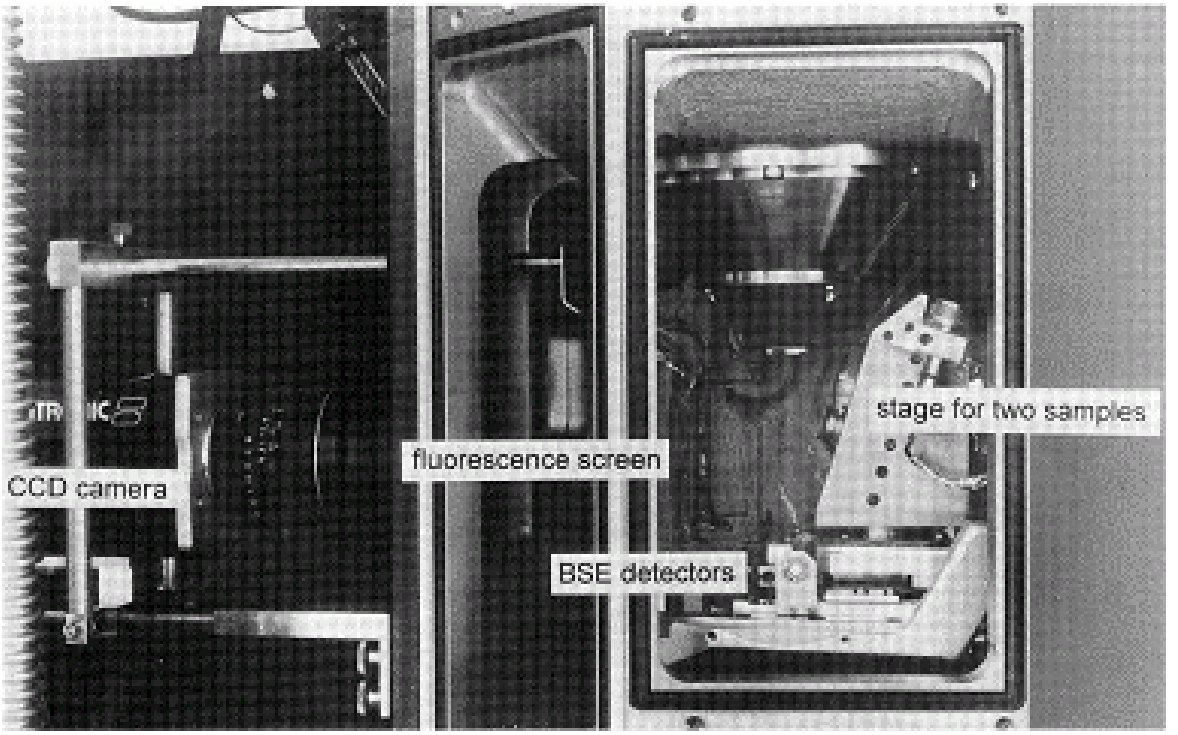

Fig. 2. Experimental set-up for the acquisition of ackscatter Kikuchi patterns with a JBOL JSM 6400 SEM.

steeply tilted to the transparent phosphor screen which is placed parallel to the primary beam. The specimen is mounted on a special motorised stage which allows *x* and *y* translations to be performed in the surface plane for alignment of the specimen area under study. The working distance is about 15 mm. The primary electron beam is focused on a grain of interest in the specimen surface and is positioned in SEM spot mode by means of the beam deflection facility, either interactively or by the computer. The microscope is interfaced to the computer via the external computer-control interface (JEOL SM-47010). The phosphor screen is viewed using an I-CCD (intensified charge coupled device) video camera (PROXITRONIC HL 5) from outside the SEM column through a lead-glass window. The screen and the camera are mounted on a sliding carriage at a fixed distance from each other. The phosphor screen is positioned some distance below the sample. Usually the screen is set close to the specimen such that the maximum intensity falls approximately at the centre of the video image. The angular range of a backscatter Kikuchi pattern is limited by the size and position of the phosphor screen. At the closest practical distance (about 2 cm), the acceptance angle in the rectangular diffraction pattern spans across a wide range of about 120° x 100°. A pattern contains several principal zone axes (Fig. 3). The phosphor screen and a cover lid are mounted coaxially on a rotary feed-through. In order to protect the screen from damage by touching the specimen or during dynamic experiments, a lid can be swung between the sample and the screen. The lid may carry a mesh grid to facilitate the alignment of the system or a filter to stop down the backscattered electrons. To give room for bulky samples in standard SEM work, the screen and the lid can be swung away.

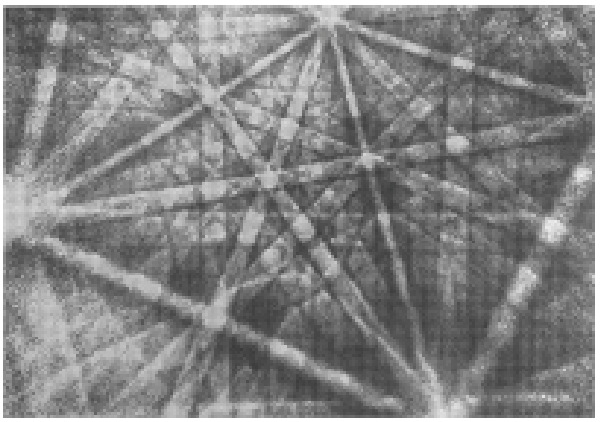

Fig. 3. Backscatter Kikuchi pattern from a copper specimen (U_{beam}=30 kV, I_{probe}=1 nA).

Often, the usual secondary and backscattered electron detectors of an SEM yield a poor image quality with steeply tilted specimens. Intensity is low and falls off rapidly with increasing detector-to-spot distance during the acquisition of an image frame, particularly at low magnifications. Some improvement is obtained by placing one or two solid-state electron detectors beneath the phosphor screen of the BKD appliance, close to the maximum of forward-scattered electron intensity (see Fig. 2). A stable signal, however, decoupled from the actual beam spot position on the specimen, is obtained by sampling absorbed rather than secondary or back-scattered electrons (specimen current) with a dedicated amplifier for forming the image. It is advisable to place a shielded pre-amplifier, commonly incorporated in a single chip, in the specimen chamber as close as possible to the specimen; this avoids the pick-up of spurious

electromagnetic signals, particularly from a turbo-molecular pump. Since the specimen current is the difference between the primary beam current and the currents of secondary and backscattered electrons, and since the number of released secondaries is usually much less than the number of backscattered electrons particularly at shallow incidence, a negative image of surface structure is obtained as compared to a backscattered electron image. While the topographical image clarity is reduced in specimen current mode, good material contrast (atomic-number contrast) and orientation contrast are usually obtained. Of course, image resolution cannot compete with secondary electron images, due to the larger volume of electron-matter interaction. However it corresponds closely to the spatial resolution obtained in backscatter Kikuchi diffraction.

Best image contrast in the diffraction patterns is obtained at high accelerating voltages (30-40 keV) and beam currents in the range of some nA. A high accelerating voltage is advantageous in many respects; the efficiency of the phosphor screen increases with electron energy. A high primary beam voltage results in a higher beam brightness and less susceptibility to interference from electromagnetic hum and magnetic or electric stray fields, particularly at large working distances. Furthermore, the primary beam can penetrate deeper into the sample and diffracted backscattered electrons originate from a thicker layer beneath the surface such that unwanted surface layers (e.g. due to oxidation or contamination, or deformation layers induced unintendedly during sample preparation) have a minor effect on pattern quality. With increasing accelerating voltage, however, the interaction volume of the primary beam increases and spatial resolution is reduced. Hence it might be of advantage to reduce the accelerating voltage for studying fine-grained materials, sputtered metallisation layers or surface coatings. With our system, the lowest practical beam voltage is 3.5 keV, which provides a spatial resolution <0.1 µm on gold. A small probe, however, demands a clean vacuum and a clean sample surface, otherwise hydrocarbons will polymerise under the beam, and contamination patches are formed.

The pattern can be viewed on a standard TV monitor. It is processed by a digital signal processor (DAGE DSP 2000) in order to improve image quality before being transmitted to the computer. Acquisition parameters are amplification, black level, brightness, gamma control, contrast and number of averaged frames. As a first step, a flat image of the background intensity is recorded, either by switching the SEM to imaging mode at a low magnification so that many grains contribute in a sequence to the pattern, or by defocusing the objective lens to the extreme. This flat image contains only background intensity, effects of non-linear camera response and unwanted patches on the phosphor screen, rather than local intensity variations due to Kikuchi bands. There are two channels, B and C, to store flat images. The actual pattern in channel A can be processed at live video frequency in the modes: subtraction of a flat background image, A - B; division (normalisation) by a flat background image, A/B = exp(ln A - ln B); subtraction and normalisation, (A - C)/(A - B). The best contrast expansion and uniformity correction are generally obtained by normalisation or by subtraction and subsequent normalisation. All functions of the digital signal processor are either set manually or controlled automatically by the computer program via the serial RS 232 interface. The benefits of a digital signal processor over a software solution (using a PC for image processing) are a much higher speed and the possibility of determining the optimum acquisition parameters by a simple interactive trial-and-error procedure before starting the program. At present, the main disadvantage of a digital signal processor is the limitation of 8-bit digitisation. This disadvantage will be overcome in the near future by frame grabber boards containing a digital signal processor of 10 or more bit digitisation.

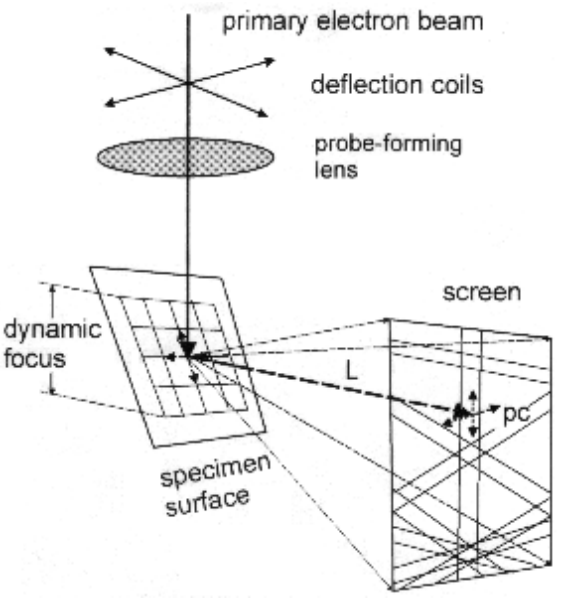

Fig. 4. Schematic view of digital beam scan in BKD showing the variations of pattern centre (pc), specimen-to-screen distance (diffraction length *L)* and focus with moving beam spot.

IV. THE CALIBRATION OF PATTERN CENTRE, CAMERA LENGTH AND SPECIMEN TILT

The pattern centre is defined as the foot of a perpendicular line from the phosphor screen to the beam spot on the tilted sample surface; it represents the centre of gnomonic projection of the pattern (Fig. 4). It is crucial to know the pattern centre with high accuracy for the correct indexing of Kikuchi bands and for the calculation of the crystal lattice orientation with respect to the reference sample directions. Unfortunately there is no mark in backscattered electron diffraction patterns which indicates exactly the pattern centre, equivalent to the primary beam spot in transmission diffraction patterns in the TEM.

Without having a backscatter Kikuchi pattern already indexed, several *interactive calibration* methods for locating the pattern centre may be used in the SEM. First of all, use can be made of the geometry of gnomonic

projection of the lattice planes via Kikuchi bands with the beam spot acting as the centre of projection. For this purpose the camera and the phosphor screen may be retracted continuously. With increasing camera length (sample-to-screen distance), a continuous increase in magnification is achieved and the live pattern 'zooms' out from the pattern centre (Hjelen *et al.,* 1993). As a simple alternative, a fine square mesh may be placed on a lid between the phosphor screen and the specimen. The shadow images of the mesh openings appear to form trapezoids with their long axes pointing to the pattern centre.

If the indexing of a pattern has already been performed and the crystal lattice orientation is known, the accurate position of the pattern centre as well as the camera length are obtained from a least square fit of the simulated band positions to the measured bands (Krieger Lassen and Bilde-S0rensen, 1993). Best results are obtained if the measured bands are located far away from the pattern centre, since their positions are most sensitively affected by the position of the pattern centre. In most cases about five bands are sufficient, and a precise calibration is obtained within a second. In the following, the last method is called *pattern fitting calibration.*

When the beam is scanning across the tilted sample, the pattern centre, camera length and working distance vary (Fig. 4). At a fixed angle of specimen tilt, however, the spot position on the sample surface is known from the *x—y* position of the spot on the viewing screen, the working distance and the image magnification of the SEM. In the initialisation file of the ORKID program, the pattern centre, the related beam position, working distance and magnification have been stored as a reference from a calibration measurement of the system. Hence for any spot position the pattern centre and camera length are readily calculated by elementary geometry at the start of a measurement, and are used in the indexing routine. In the following, this procedure is called *auto calibration.*

For very low magnifications there may be a slight deviation of the calculated from the true values of the pattern centre and the camera length. The program, however, starts with a very close estimate, such that it is always feasible to use the pattern-fitting calibration procedure for additional fine-tuning. In effect the user no longer has to bother about the pattern centre when varying the spot position, specimen height or microscope magnification, or when changing the specimen. Only after disassembling the system (with a change in the positions of the camera or the phosphor screen) must one of the interactive calibration procedures be carried out and the new reference values stored in the initialisation file.

The angle of specimen tilt is calibrated by using a (100) silicon crystal as a test specimen. For a tilt angle of 19°30' between the specimen surface and the primary beam direction, the (114) pole falls on the pattern centre in a direction normal to the optic axis, and for a tilt angle of 35°16' the (112) pole direction is normal to the optic axis, i.e. normal to the direction of the undeflected primary beam. Hence the actual specimen tilt can readily be obtained from the spacing between the pattern centre and the (114) or the (112) pole, respectively.

V. DYNAMIC FOCUSING UNDER SOFTWARE CONTROL

The fact that SEMs are characterised by small aperture angles a of the beam spot results in a large depth of focus D_f. A sharp image occurs within a finite distance above and below the object plane as given by $D_f=\delta/\tan\alpha$ where δ is the smallest spacing of two resolved details in the specimen. Spatial resolution in backscattered electron diffraction is about 0.5 μm or less. But large beam apertures (10^{-3} rad or more) have to be used and the specimen surface has to be highly tilted with respect to the primary beam for generating a sufficiently intense BKP. Hence only a narrow strip of the specimen surface, typically a few tenths of a millimetre wide, is in focus. With fine-grain material or at low magnifications, dynamic focusing is indispensable for ACOM operation with digital beam scan.

Dynamic focusing by software rather than by SEM hardware has been implemented in the ORKID program, since hardware appliances for dynamic focusing are not available for all SEMs, or in some SEM versions may only work correctly for a specimen tilted about the stage axis or for a limited range of specimen tilt, magnification and working distance not sufficient for BKD. The actual working distance is calculated for the *x-y* spot positions either from reference values in the initialisation file in a similar way as the pattern centre is obtained in autocalibration, or interpolated between the focus settings at the start and end points of the scanned field in ACOM mode. Whenever the spot passes to the next raster scan line and the working distance has changed, the current through the objective lens is adjusted by the computer. For this technique the SEM lens and scanning control has to be interfaced with the computer for data tranfer in both directions (Fig. 5). Since scanning speed in ACOM mode is relatively slow, the impedance of the objective lens does not interfere with dynamic focus setting by the computer, and hence an additional low-impedance lens coil is not required for dynamic focusing. If the camera is mounted at an oblique angle with respect to the tilt axis of the specimen stage, a scan rotation appliance may be convenient in order to enable the scanning frame to be aligned with the specimen *x-y* translation.

VI. THE INTERACTIVE MEASUREMENT AND INDEXING OF BACKSCATTER KIKUCHI PATTERNS

Our computer program for interpreting backscatter Kikuchi patterns (Schwarzer *et al,* 1996) is in essence a reduced and modified version of ORKID/TEM which

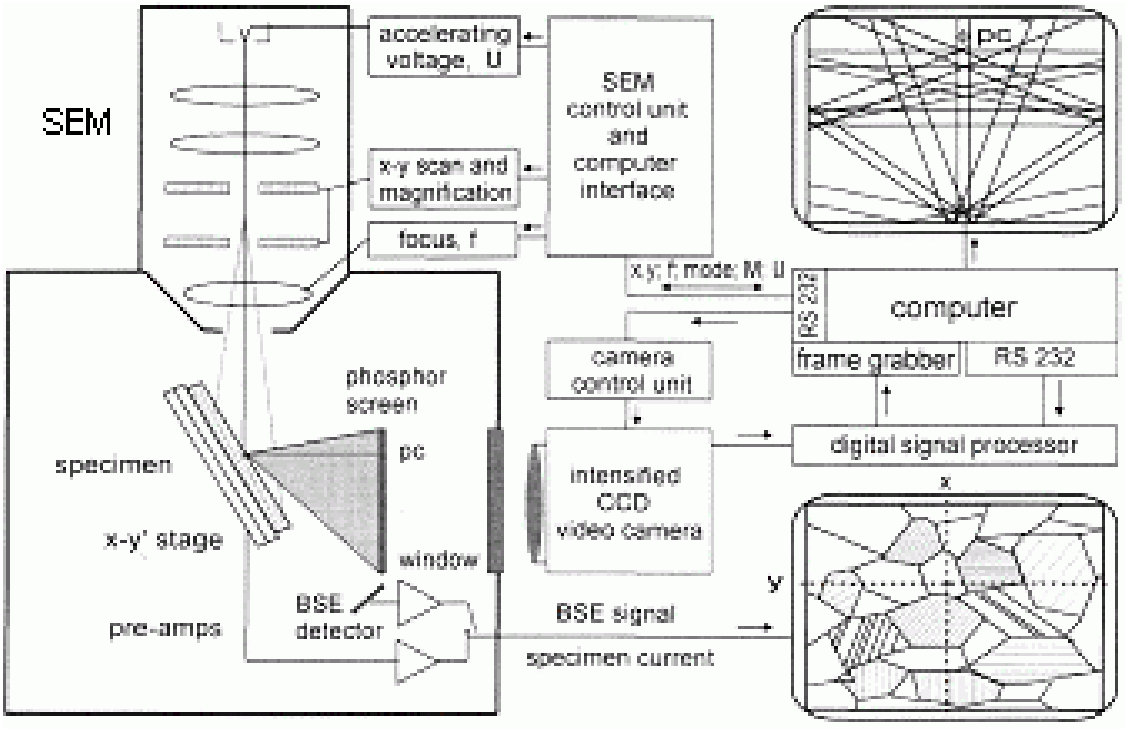

Fig. 5. Fully computer-controlled SEM for automated crystal orientation mapping.

enables the automated interpretation of transmission Kikuchi patterns as well as electron diffraction spot patterns on a TEM (Zaefferer and Schwarzer, 1994a; Zaefferer, 1996). It is written in 32 bit code C++ language for Windows® 95. The modules for the interpretation of spot patterns and interactive determination of Burgers vectors and glide systems (Zaefferer and Schwarzer, 1994b; Schwarzer and Zaefferer, 1995) have been omitted, while supplementary calibration routines have been added. The SEM driver has replaced the interface routine with the TEM and a simpler Hough-Radon transform routine for the automated extraction of band positions is used. The convenient simulation of sample tilt, by displaying simulated Kikuchi patterns and stereographic projections on the computer screen, is still available.

In general, the positions of at least three bands and the pattern centre are required for the interpretation of a Kikuchi pattern. Indexing is performed either by considering interplanar angles only or by considering interplanar angles *and* the ratios of interplanar spacings. Calculations of interplanar angles and spacings are performed in a fast, simple and uniform way for all crystal symmetries of the Laue group by transforming the reciprocal lattice vectors, $\mathbf{g}(hkl)$, into an orthonormal coordinate system, $\mathbf{g}^{\circ}(hkl)$, by matrix multiplication with the inverse crystal matrix, $\mathbf{A}^{-1}$:

$$\mathbf{g}^{\circ}(hkl) = \mathbf{g}(hkl) \cdot \mathbf{A}^{-1} \qquad (2)$$

with the crystal matrix $\mathbf{A}$:

$$\mathbf{A} = \begin{pmatrix} a & b\cdot\cos\gamma & c\cdot\cos\beta \\ 0 & b\cdot\sin\gamma & c\cdot(\cos\alpha - \cos\beta\cdot\cos\gamma)/\sin\gamma \\ 0 & 0 & c\cdot[1+2\cdot\cos\alpha\cdot\cos\beta\cdot\cos\gamma-(\cos^2\alpha+\cos^2\beta+\cos^2\gamma)]^{1/2}/\sin\gamma \end{pmatrix}$$

a, b, c, α, β and γ denote the crystal parameters of the unit cell (Schumann, 1979). The calculation of interplanar angles, $\angle\,[\mathbf{g}(hkl)_1, \mathbf{g}(hkl)_2]$ and spacings, J_{hkl}, is thus reduced in orthonormalised space to:

$$\angle\,[\mathbf{g}(hkl)_1, \mathbf{g}(hkl)_2] = \arccos\,[\mathbf{g}^{\circ}(hkl)_1 \cdot \mathbf{g}^{\circ}(hkl)_2] / [|\,\mathbf{g}^{\circ}(hkl)_1 \cdot \mathbf{g}^{\circ}(hkl)_2\,|] \qquad (3)$$

$$1/d_{hkl} = (\,\mathbf{g}^{\circ}(hkl)_1 \cdot \mathbf{g}^{\circ}(hkl)_2\,)^{1/2} \qquad (4)$$

Since transformation (2) and the spacings calculation (4) are carried out only once for a crystal structure and then stored in the computer memory in the form of a look-up table, only the interplanar angles (3) have to be calculated during the indexing procedure. Execution time is further reduced by checking cosines rather than angles, thus avoiding the calculation of the inverse cosine in (3).

With high-symmetry crystal lattices, the effort of measurement can be reduced since the positions of the centre lines are sufficient; indexing can be done without knowing the band widths. The centre lines correspond to lines of intersection of the (imaginarily extended) diffracting lattice planes with the phosphor screen, and hence yield their interplanar angles. Fortunately the distribution of interplanar angles is discrete and extremely sparse, particularly with cubic, tetragonal and hexagonal crystal symmetry, and a unique indexing is almost always possible by simply sorting out a consistent set of interplanar angles. For lower crystal symmetry, the positions of the Kikuchi lines bordering

the bands are required. The interplanar spacings are then available from the Kikuchi band widths knowing the Bragg angle; the interplanar angles are deduced from the centre lines of the bands. Since a backscatter Kikuchi pattern comprises a large angular range with several low-index zone axes (Fig. 3), it is usually sufficient to make allowance for only the first three or four families of low-index crystal lattice planes to enable a correct pattern interpretation, e.g. the [110], [200], [211] and [220] planes are considered for bcccrystals and the [111], [200] and [220] planes for fee crystals.

The digitised diffraction pattern to be indexed is passed on to the random-access computer memory, either live from the camera or read from a file as a stored PCX image, and displayed in a window on the computer monitor. Interactive orientation measurement is straightforward. For the interpretation, the operator has to mark either the coordinates of the centre lines *(centre-line method)* or the Kikuchi lines *(band width method)* of at least three bands with the cursor on the monitor screen. The indexing routine is described in detail elsewhere (Zaefferer and Schwarzer, 1994c). Sometimes more than one crystallographically non-equivalent set of indexing of the bands is in accord with the measured band positions. Reasons for finding false solutions may be coincidence orientations for the selected bands, bands taken only from one zone axis, inaccurately measured bands, too large error limits, a false crystal symmetry, or a badly misaligned system. From the indexed bands and the actual position of the pattern centre, the crystal lattice orientation with respect to the specimen normal and x stage direction is calculated.

The more bands are indexed consistently, the more likely it is that a correct solution has been found. Usually between 4 and 8 bands are considered. If they failed in indexing, successive bands can be skipped until at least three bands are left over. The ratio (number of consistent bands/all measured bands) serves as a confidence-level indicator.

All orientations of a grain which are consistent with the measured band positions (or optionally down to a chosen confidence level) are stored in a buffer for further visual inspection. In order to exclude false solutions and to make a decision between [*uvw*] and directions in cases where only two bands (or only bands belonging to a common zone axis) had been entered, a simulated Kikuchi pattern is calculated for the candidate solution and overlaid on the experimental Kikuchi pattern. If the simulated pattern does not fit, the operator may request the next calculated orientation from the buffer; its simulated pattern is displayed and examined until a correct solution is found or the stock of candidate solutions is exhausted. In the latter case, the measurement has to be repeated and another combination of bands entered. With a well calibrated system, more than 95% of the first-displayed solutions are correct, i.e. those with the highest confidence level. However, if only bands with a common zone axis have been measured, every second solution is likely to be false unless a mirror plane is present. The grain orientation is displayed on the monitor screen in (*hkl*)[*uvw*] notation for the specimen normal direction and the reference x-direction in the specimen surface. The result of orientation measurement can be stored on an ASCII file in the form of the (orientation) **g** matrix or the Euler angles, optionally along with further acquisition parameters such as the running number of measurement, the x-y spot position, or commentary text.

VII. FULLY AUTOMATED MEASUREMENT AND INTERPRETATION OF BACKSCATTER KIKUCHI PATTERNS

The interactive measurement of band positions is tiring and takes up to one minute per grain orientation, so it is mainly used for initial calibration of the system, for final inspection of those specimen locations where automated pattern interpretation has failed, or for superimposed patterns from abutting grains. Very crisp patterns, particularly from refractory metals and some minerals, may exhibit sharp (high-order) lines which interfere with the automated detection of band positions, as described in the following. Then the situation is similar to sharp transmission Kikuchi patterns in the TEM, which require a special processing and modified filters for locating peaks in the Hough-Radon transform (Zaefferer and Schwarzer, 1994a). With lower crystal symmetry, bands and lines become increasingly dense and overlaid. Interactive measurement, preferably of Kikuchi line positions (i.e. the "band-width method" which evaluates the positions *and* the widths of the bands), including a check of the results by visual comparison of the experimental pattern with an overlaid simulated pattern, is a still more reliable technique in these cases.

The automated extraction of band positions in a Kikuchi pattern by using a modified, intensity-weighted Hough algorithm has proved to be very stable, particularly for patterns from high-symmetry crystals (Krieger Lassen *et al.,* 1992). The Hough transform (Hough, 1962) is essentially a discrete version of the more general Radon transform (Radon, 1917). A straight line in the pattern can be parameterised by its distance ρ_l from the origin of an x-y reference frame and the angle φ_l made between its normal with the x axis within the interval $[0;\pi]$:

$$\rho_l = x_l \cos\varphi_l + y_l \sin\varphi_l \qquad (5)$$

This relation transforms all points (x_i, y_i) on the line into a single point (ρ_l, φ_l) in Cartesian (ρ, φ) Hough space. In contrast to the original concept of Hough, which only considers binary values for accumulation, real intensities are summed up here and are finally normalised, i.e. divided by the number of points along the line. A bright line in the real diffraction pattern is marked out as a peak in Hough space, which is easily

detected in a search routine. In our program the Hough-Radon transform is normalised to the stored Hough-Radon transform of a flat image, instead of dividing each peak individually by the number of points contributing to the line under consideration. The benefits are a higher numerical speed and compensation for any artificial peaks or biasing caused by the finite size and rectangular shape of the input diffraction pattern. The cos φ and sin φ values have been calculated in advance and stored in a look-up table.

So far the intensity-weighted Hough-Radon transform is nothing else than the mathematical description of a standard slit densitometer scanning across a diffraction pattern whereby the micrograph is rotated step by step after each pass. If the intensities are plotted in Cartesian (*m, c*) space, the more familiar slope-intercept parameterisation of a straight line is obtained:

$$y_i = m_l x_i + c_l \tag{6}$$

To avoid the singularity for vertical lines, the slope (m) can be limited to the interval [-1, 1], and y can be interchanged with x for the steeper lines. There are many other parameterisations for the Hough-Radon transform in order to detect straight lines as well as arbitrary shapes. The reader is referred to Illingworth and Kittler (1988) and Bässmann and Besslich (1993) for more details. The common algorithm for extracting Kikuchi band positions is based on relationship (5).

A real backscatter Kikuchi pattern is mainly composed of broad and often diffuse excess bands. Sharp excess and defect Kikuchi lines and Kikuchi envelopes—which are a characteristic feature of transmission Kikuchi patterns—exist only in backscatter Kikuchi patterns from a virtually perfect volume of diffracting crystal, recorded with a high-grade camera system. The Hough-Radon transform, however, maps a broad band in real space into a "butterfly-shaped" peak (rather than into a sharp point) in Hough space. The spread of the butterfly is a measure of the band width, i.e. of the Bragg angle. In order to locate the centres of these peaks, a matched convolution filter is applied. The performance of the algorithm depends significantly on the shape of the filter mask. It is advisable to use different masks for broad bands (i.e. for low accelerating voltages and high-index bands) and narrow bands. The peak coordinates yield the centre-line positions of the Kikuchi bands in the diffraction pattern, as stated by equation (5). They are listed according to their relative intensities and passed on to the indexing subroutine. As a rule, a high excess-band intensity is linked with low indices of the related lattice planes. There are often much more than a dozen bands detected automatically in a Kikuchi pattern, some of which can hardly be perceived by visual inspection. So the user may limit, according to their intensity, the number of bands to be used for indexing. The main advantage of the Hough procedure is its robustness and low sensitivity to image noise. Optimisation of the Hough algorithm for backscatter Kikuchi patterns is discussed in great detail by Krieger Lassen (1994). The shape of the "butterfly" peaks is used to advantage in some cases for making a distinction between narrow and broad bands.

Automated computer analysis of backscatter (and transmission) Kikuchi patterns has now replaced the interactive measurement in most applications. The operator has simply to select the grain of interest by positioning the beam-spot cursor on the SEM image, press the mouse key for automated pattern capture and interpretation at this grain position, and finally check the overlay image of the measured and simulated Kikuchi patterns for correctness. With autocalibration enabled, the user need not pay attention to image magnification or working distance, nor keep the actual beam spot position within some small range. The accelerating voltage is automatically transmitted from the SEM to the computer program as a further microscope parameter. It is used for choosing the appropriate "butterfly mask" in the Hough routine and required for correct drawing of the band widths in the overlaid simulated Kikuchi pattern.

VIII. AUTOMATED CRYSTAL LATTICE ORIENTATION MAPPING (ACOM)

The final step of automation in orientation measurement with an SEM is reached with the integration of a computer-controlled selection of the probed spots on the specimen. There are different approaches locating the measured spots: either the specimen is translated with respect to the stationary primary beam in the x and y directions using a computer-controlled high-precision specimen stage (Adams *et al*, 1993) or the primary beam is moved, step by step under computer control, across a stationary specimen surface (Schwarzer and Kunze, 1995) as in conventional scanning electron microscopy. The measured spots may be some selected individual points, they may form a dotted line or fill a raster field on the specimen. The computer-controlled digital beam scan, as realised in the ORKID program, uses the natural operating mode of an SEM: the specimen area under consideration is first inspected with the SEM in conventional imaging mode at an appropriate magnification. The image is then kept in the digital frame store for continuous display, a standard facility in a modern SEM. Finally, the microscope is switched to spot-mode operation and the image cursor on the display monitor is positioned on successive grains of interest, either interactively (for individual grain orientation measurement by the operator) or by the computer (for automated crystal lattice orientation mapping).

For ACOM, our microscope is interfaced to the computer (Fig. 5) via an external computer-control interface (JEOL SM-47010). Since only 8 bits are available in this commercial appliance, a separate 12-bit digital-to-analog converter interface has been added to the SEM scan generator for beam positioning. Of course, a raster of 4096 x 4096 addressable grid points (provided by the 12 bit DAC) is not a realistic number of

image points acquired with present computers and camera systems. The fine-meshed raster grid, however, enables a very precise setting of measured spots on the tilted specimen surface, by interpolation. Since image resolution of an SEM depends on the spot size of the beam rather than on the actual magnification, a high spatial resolution is attainable even at a low magnification, provided the grid is sufficiently dense and dynamic focusing is enabled. Thus, distant surface regions can be imaged in sequence without having to translate the sample.

The primary-beam spot follows synchronously any movement of the cursor by means of the standard beam-deflection device. It is, however, important to check that there is no shift between the cursor position in the stored image and the related beam-spot position on the specimen surface when switching to spot mode operation. A simple check of this synchronism is performed by slowly moving the cursor across a grain boundary in the microstructural image and watching the expected change of related Kikuchi patterns. For some microscopes it might be necessary to record the micrographs exclusively at slow scan rate before freezing the image in the frame store, or to have the beam deflection circuits recalibrated.

To resume automated crystal lattice orientation measurement with the ORKID program, the operator has to switch to an appropriate image magnification, select the sample area of interest and enter the points or field to be measured. The raster field for area scan is defined by marking, with the cursor in the stored image, the start and end points of a rectangular field or n polygon points, respectively. Finally, the user has to focus the image or the diffraction patterns on the top and then on the bottom scan line of the imaged field. In the same procedure, the pattern centres for the start and end points can be fine-tuned by pattern-fitting calibration in order to override the values calculated by autocalibration. Fine-tuning is not required for magnifications above about 500 times , since autocalibration is then adequate. The actual (x, y) positions bounding the scanned field and their working distances are thus measured and transmitted to the computer memory as reference values to be used later on for dynamic focusing and autocalibration by the software. For the unattended high-speed measurement of a reduced number of individual grain orientations, such as during dynamic experiments, the beam spot is positioned on the specimen by the computer either from point to point (out of a preselected set) or along a straight line between two end points which had been marked in a similar way as with an area scan. Finally, the microscope is automatically switched to spot mode, the primary beam spot is focused and positioned on the start point, and automated lattice-orientation measurement is carried out. While scanning across the sample, the software instructs the system to perform in sequence the beam scan, dynamic focusing and autocalibration by linear interpolation between the start and end-point reference values, pattern capture, adjustment of signal amplification or capture of another flat image (if found necessary), pattern interpretation and finally the storage of the grain orientation in every point (x, y).

There are several options implemented to control unattended measurement. First, the background may change excessively when the beam scans across a large field on the sample, particularly at low magnifications. Hence the program allows for the automated acquisition of a new flat image into channels B or C of the digital signal processor after a pre-set number of measured image points. Second, if successive patterns could not be indexed automatically, either the background or the image intensity (i.e. the primary beam current) may have changed too much. Therefore the mean intensity of the last pattern is calculated, and—if this value is out of range of a pre-set tolerance value—the signal amplification on the digital signal processor is adjusted by the computer. Otherwise a new flat image is recorded and the measurement is repeated. If indexing fails again, these image spots are marked and their x y coordinates are stored for further inspection by the operator. In the latter cases, the primary-beam spot might have fallen upon a grain boundary so that two patterns are superimposed which could not be indexed automatically, or else there is a second phase, a precipitate or an artifact in the surface (etch pit, steep topography, excessive local deformation, etc.).

The speed of ACOM has been increased noticeably by a dual-task operation: while a pattern is interpreted by the computer, the primary beam is positioned on the next image spot, the camera is switched to recording and the new pattern is processed digitally and kept ready on the DSP to be transmitted to the computer. The time elapsed for one point is less than half a second on the average for a 200-MHz Pentium Pro PC. About 5000 grain orientations per hr can be acquired from rather diffuse patterns, and more than 10,000 grain orientations have been measured per hr with sharp patterns from recrystallised fcc metals.

The resulting database may be used in supplementary programs, e.g. for the calculation of the orientation distribution function (ODF) or misorientation distribution function (MODF), pole figures, local materials properties, or for a graphical representation of the microstructure by marking the sampled points of the grains in a map by colours specific to the lattice orientations or misorientations across grain boundaries (Gerth and Schwarzer, 1993). Since an orientation comprises three independent variables, a compressed version of the parameter is calculated by assigning a stained RGB (red, green, blue) colour to a sample direction in the crystallographic standard triangle, or to the orientation in three-dimensional Euler or Rodrigues space. These "stained glass" micrographs are named "orientation images" or more precisely "crystal orientation maps" (COM). Two maps generated from two sample reference *directions* in the (*hkl*)[*uvw*] notation are required of the same area for a full description of the grain *orientations,* whereas a single map is sufficient with Euler angles or Rodrigues vectors as orientational parameters.

In the crystal orientation maps, areas of similar orientation are shown in similar colours so that orientational components of the microstucture are accurately revealed.

Orientation imaging microscopy (Adams *et al,* 1993), by translating the specimen mechanically in an *x-y* stage step by step along its surface, is a less complicated procedure than the digital beam-scan ACOM technique described above, since the primary beam is kept stationary. There is no need for rectifying distortions of the scanned field, refocusing the objective lens, or for recalibrating the pattern centre or diffraction length. The digital beam-scan technique (Schwarzer and Kunze, 1995), however, offers some significant advantages over a scanning specimen stage: it is cheap, fast, reliable, precise and easy to operate. Special specimen stages dedicated for dynamic experiments (e.g. heating stage, cooling stage, tensile stage) can be accommodated conveniently. Additional features can be implemented in the software package. So ACOM by scanning the beam across the sample may become the common technique in the near future. Commercial systems have been developed lately. They still lack, however, autocalibration and dynamic focus control by the software.

IX. SPECIMEN REQUIREMENTS

Specimen preparation for BKD study is generally straightforward, but beam-sensitive and high-resistivity materials require special treatment (Schwarzer, 1993b, 1994b). A specimen for backscattered electron diffraction must first be suitable for investigation in an SEM; in particular it must withstand a high vacuum and exposure to a beam of energetic electrons. Secondly, it has to be crystalline with grains exceeding some tenths of a micron in size. Heavy plastic strain and foreign layers on the surface are prohibitive. The preparation of metal specimens may be difficult, since unwanted plastic deformation or artifacts in the surface layer can hardly be avoided with ductile materials, and the probed crystal volume is then no longer representative of the bulk. The diffuse backscatter Kikuchi pattern might be interpreted erroneously as being related to a deformed sample, because the diffuseness of the bands is usually a measure of local plastic strain.

Special precautions are necessary when cutting and polishing soft samples with abrasives. Often the same techniques can be used as for optical microscopy. A final deep chemical etch is recommended in order to remove deformed layers from the surface. Chemical-mechanical polishing is particularly favourable whereby an etching reagent is deliberately incorporated in the abrasive slurry (colloidal alumina or silica) in order to remove continuously from the surface any protective reaction products of etching as well as strained layers. Surfaces polished in this way show a slight but much more uniform etching than it would have been obtained if the specimen had only been immersed in the etching or polishing reagent. With conductive single-phase materials, best results are usually obtained with chemical or electro-chemical final polishing. A slight ion-milling at grazing incidence of the low energy ion beam may be applied in order to remove contamination layers (etch residues, reaction/oxidation products) from the surface. The preparation of brittle materials such as ceramics, minerals or intermetallic compounds is easier. Polished sections after a gentle etch and clean fracture or cleavage surfaces can readily be studied. Specific difficulties are encountered in the examination of high-resistance or sensitive materials. A thin evaporated carbon layer may result in diffuse patterns, in which case a higher beam voltage is recommended to increase the penetration of the beam through the surface layer. There are several experimental techniques available which reduce the electrical resistance of the specimen, reduce the probe-current density, increase the secondary electron emission coefficient or compensate for surface charge (Schwarzer, 1994b).

X. APPLICATIONS OF BACKSCATTER KIKUCHI DIFFRACTION

The strong point of backscatter Kikuchi diffraction with the SEM is the combination of lattice orientation with microstructural features at user-defined specimen areas and sub-microscopical resolution. The knowledge of crystal-lattice orientations and their statistical distribution, expressed by the orientation distribution function (ODF) (Bunge, 1982) is valuable in itself, since many material properties are anisotropic. Their (average) values and directional dependence in a sample can, in principle, be calculated from the ODF. Even more revealing is a grain-specific investigation of the microstructure, rather than a statistical approach such as the representation of crystal texture by pole figures or the ODF. Lattice orientations may vary specifically from place to place during the production or use of a workpiece. Furthermore, material properties may change discontinuously across grain boundaries, and the type and density of grain boundaries may significantly affect the behaviour of a material. Misorientations across grain boundaries are directly available from the measurement of individual grain orientations.

The "character of a grain boundary", according to the coincident site lattice (CSL) model (Bollman, 1970), does not sufficiently account for the real structure of a grain boundary. The Σ value in this notation is the reciprocal fraction of common lattice sites of two (imaginarily) interpenetating lattices and, hence, is in essence a simplified description of the misorientation between two abutting grains, in terms of a single parameter (Σ) rather than using three orientational parameters ($\Delta\mathbf{g}$). The CSL model has been widely used in the past. Special Σ values seem to be correlated with special properties, although a given low-Σ misorientation can have many different boundary planes. This experimental finding can be explained by the tendency of low Σ values to be correlated with a preferred

occurrence of special (in particular symmetric) grain boundaries which share a large fraction of common lattice sites. It is also possible that macroscopically asymmetric grain boundaries may dissociate into microscopic sections of piecewise-symmetric facets of symmetric grain boundaries. It is worth mentioning that, even in a (symmetric) grain boundary, a pronounced directional anisotropy of properties may appear.

A more complete crystallographic description of a grain boundary requires, in addition to the specification of the grain misorientation $\Delta\mathbf{g}$, the grain boundary normal direction $\mathbf{n}$, expressed for example by two directional parameters with respect to one of the crystal lattices (Randle, 1993). Hence 5 parameters have to be determined experimentally. The spatial orientations of grain boundary planes can often be obtained by simply comparing the grain micro structure in the images of the top and back sides of thin samples, or in images after consecutive sectioning. This is performed by removing thin slices, one after the other, from the surface, e.g. by careful grinding and polishing. A standard metallographic technique for monitoring the depth of grinding is to control the decreasing sizes of microindentation pyramids punched in the initial surface. When the spatial orientations of the grain boundaries are known, their normals $\mathbf{n}$ can readily be indexed crystallographically, since both grain orientations are known from orientation measurement. The misorientation matrix (whose nine elements contain three orientation paramers in a linearly dependent form) describes the rotation of one grain into the orientation of the other one. It follows simply from multiplication of the orientation $\mathbf{g}_1$ of the first grain with the inverted orientation matrix $\mathbf{g}_2$ of the other grain: $\Delta\mathbf{g}=\mathbf{g}_1\cdot\mathbf{g}_2^{-1}$. The misorientation $\Delta\mathbf{g}$ must not be mistaken for the distance ω between two grain orientations $\mathbf{g}$' and $\mathbf{g}$" expressed for instance by their Euler angles (φ_1', Φ', φ_2') and (φ_1", Φ", φ_2") (Helming *etal,* 1996):

$$\cos\frac{\omega}{2} = \cos\frac{\varphi_1'-\varphi_1''}{2}\cos\frac{\varphi_2'-\varphi_2''}{2}\cos\frac{\Phi'-\Phi''}{2} - \sin\frac{\varphi_1'-\varphi_1''}{2}\sin\frac{\varphi_2'-\varphi_2''}{2}\cos\frac{\Phi'+\Phi''}{2} \quad (7)$$

Experimental errors of grain orientation and normal direction measurement are typically in the range of one or a few degrees, respectively. This is often sufficient for the analysis of crystallographic texture. A detailed study of misorientations or the distribution of special grain boundaries, however, might demand a higher precision. Then the Kikuchi technique in the TEM is superior. With the availability of automated grain-orientation measurement in the SEM, it is now readily feasible to acquire a statistically significant database for the characterisation of crystallographic texture, misorientation and grain boundary normals on a grain-specific level. By the combination of consecutive sectioning and ACOM, a three-dimensional reconstruction of the microstructure including the grain boundary orientations becomes feasible.

The true structure of a grain boundary (including the specification of spatial translations of the two abutting lattices with respect to each other and the positions of individual rows of atoms in the boundary) may be revealed by high resolution TEM in combination with contrast simulations. This technique, however, is limited to a few special cases where the grain boundary plane as well as a low-index zone axis in each grain can simultaneously be aligned parallel with the primary beam direction. Furthermore, the specimen has to be extremely thin for high resolution lattice imaging, so specimen preparation and significance of the sampled region—possibly doubtful for characterising the whole workpiece—may be other drawbacks. Individual grain-orientation measurement does not suffer from these limitations.

There are promising new applications in materials science beyond local texture analysis (Randle, 1992, 1993) which are now amenable to the automated Kikuchi technique: image contrast in a crystal orientation map is unambiguously related to the true grain orientations. A stereological evaluation of a crystal orientation map may reveal morphological parameters (e.g. grain size, shape, arrangement, number of boundaries of a grain) which are often hardly accessible due to an uncertain or missing contrast between grains in conventional LM or SEM images. The diffraction pattern contains the symmetry of the crystal system (cubic, hexagonal, etc.). Hence phases, irrespective of their chemical composition, can be discriminated if they have a different crystal symmetry (e.g. bcc (ferrite) from fcc (austenite) iron, or some oxides, carbides or nitrides). Very crisp patterns obtained with a high-grade camera system may even enable a precise phase analysis (Michael and Goehner, 1993). The diffuseness of a Kikuchi pattern is a measure of local dislocation density. The pattern quality can so be used as an additional quantity to map the spatial distribution of local deformation (e.g. strains associated with welds, Adams *et al,* 1993). Some work, however, has still to be done to improve the strain assessment to a quantitative analytical technique. Of particular value will by dynamic in-situ ACOM studies of recrystallisation and grain growth, or fracture, creep and fatigue experiments by using a heating, tensile or cooling specimen stage.

A rapidly expanding application of ACOM to thin films and microelectronics is expected, since the grain size of metallisation layers is in the range of the interconnect dimensions, hence crystallographic effects are becoming increasingly important. The reader is referred to proceedings of the international conferences on textures of materials, ICOTOM-10 (1994) and ICOTOM-11 (1996), for recent progress in the field of materials characterisation.

XI. EXAMPLE OF ACOM APPLICATION

Thin layers of polycrystalline metals or non-metals as used for microelectronic devices usually contain

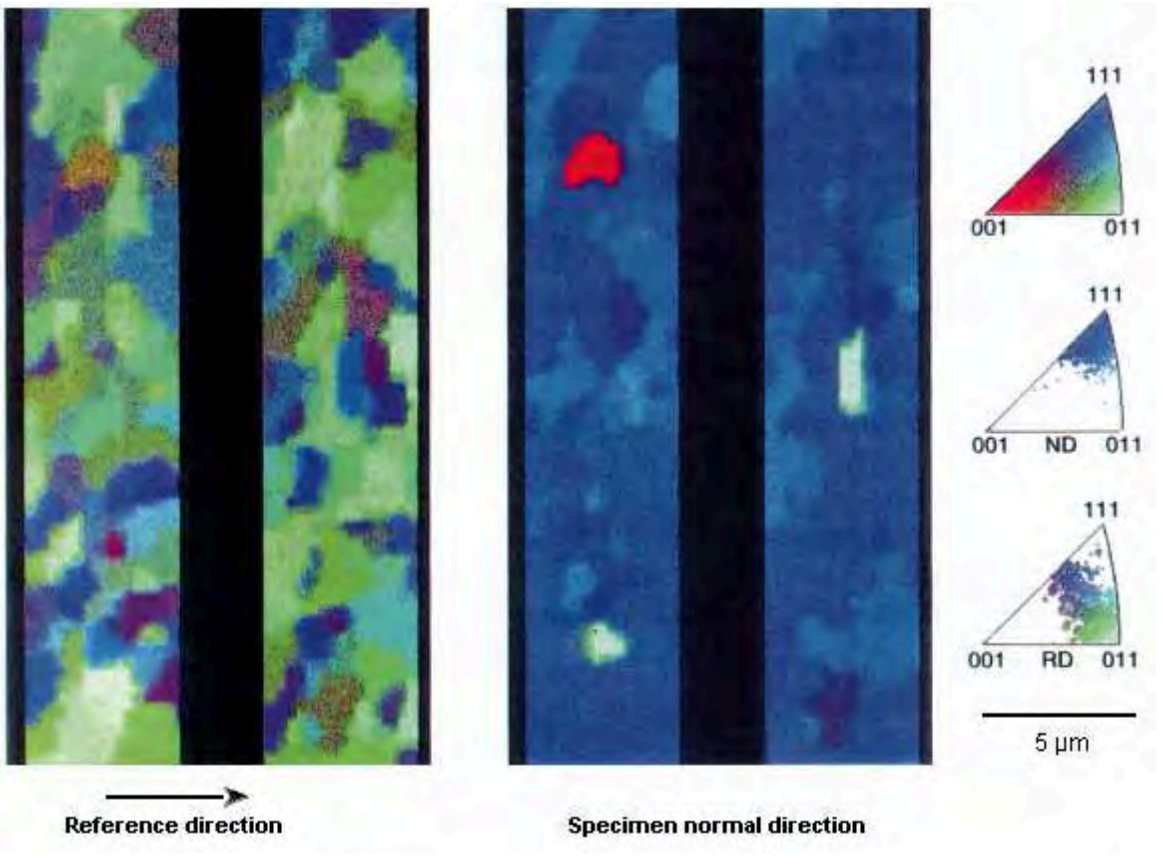

Fig. 6. Crystal orientation maps of aluminium interconnect lines on a SiO_2/Si substrate (left: reference direction normal to the interconnect line; right: reference direction normal to the layer surface).

preferred crystal orientations. Thin films deposited on a solid substrate by sputtering or evaporation under high vacuum or by electroplating often exhibit a marked fibre texture, i.e. most of the grains have a common crystallographic direction aligned in parallel with a macroscopic direction, for instance the sample normal. A reliable prediction of crystallographic texture, however, is difficult since it depends in a complex manner on many parameters of the production process such as interfacial energy and lattice misfit between the deposited film and the substrate, free surface energy, strain energy, surface, grain boundary and volume diffusion, grain boundary mobility, residual gas atmosphere and temperature. Furthermore, crystal texture may change during use of the circuit as a consequence of thermomechanically-induced local stress (Gerth *et al.,* 1994) and recrystallisation.

A particular problem of present microelectronic technology is the failure of metal interconnects in integrated circuits due to unwanted mass transport by electromigration or thermomechanical growth of hillocks. Figure 6 shows an ACOM image of two initial interconnect lines in an electromigration test specimen. The aluminium layer of 0.75 µm thickness had been sputter-deposited onto an oxidised silicon single crystal substrate and patterned as parallel lines 5 µm wide. The interconnect lines had to be placed in a vertical direction for measurement in the SEM. Hence dynamic focusing under computer control was essential to resolve the fine grain structure. If the interconnect lines were placed horizontally, focus could be kept constant across the narrow lines, but a large fraction of electrons scattered from the metallisation layer were incident on the silicon oxide support and gave rise to excessive specimen charging. The left COM represents by specific colours the crystal orientations in a direction normal to the interconnect line: the right COM represents the orientations in specimen-normal direction. The latter image demonstrates a sharp fibre texture along the specimen-normal direction, since nearly all grains are represented by the same blue colour that represents a <111> crystal direction (see colour key) while in the left image no preference for a crystal direction in the layer plane can be seen. The individual grains are clearly distinguished from each other b,y various colours. The grains show some colour variations due to small-angle grain boundaries, indicating some localised mechanical stress within the larger grains which has not yet been relaxed.

In a similar way, the misorientations across grain boundaries can be represented by colour maps constructed from ACOM measurement. Figure 7 shows the same section of aluminium interconnect lines. As parameters, the misorientation angles (left map: blue for angles 8°; red for angles 35°) and the crystallographic directions of the rotation axis with the smallest rotation angle (right map) have been chosen. From these maps,

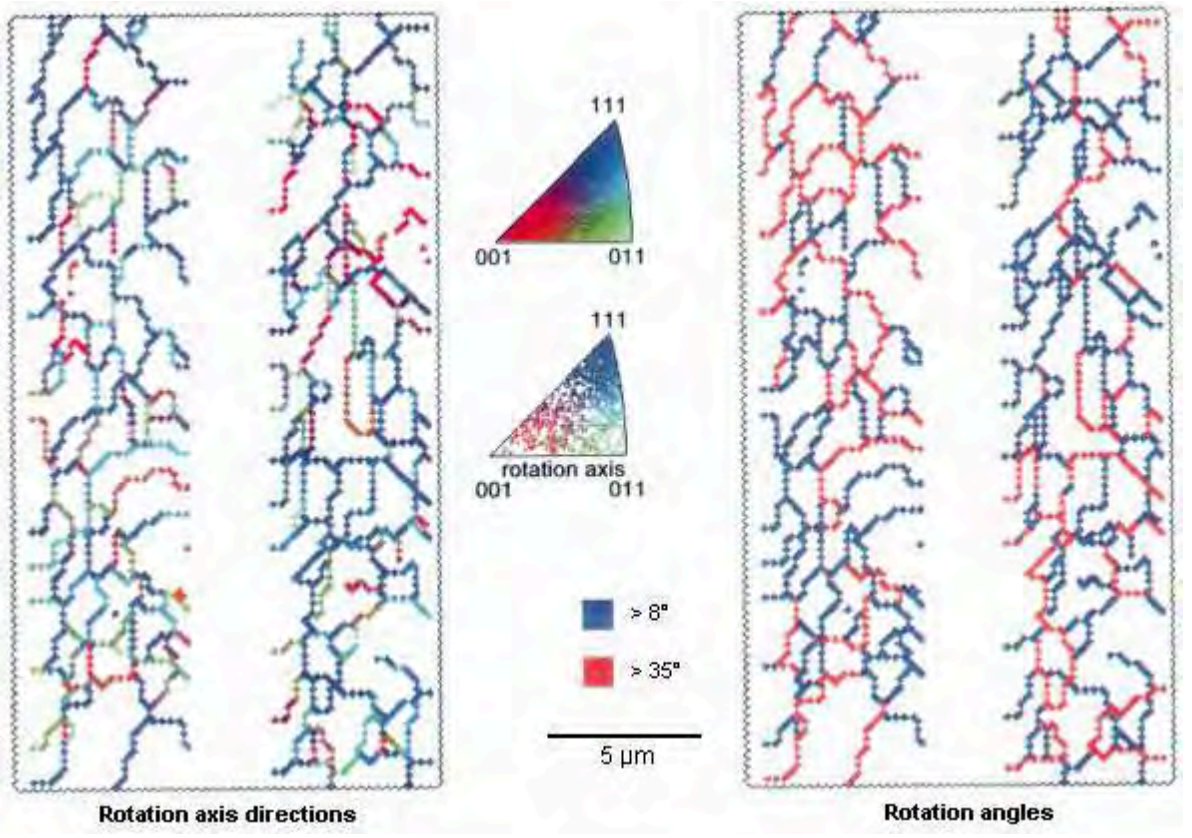

Fig. 7. Grain boundary misorientation maps of aluminium interconnect lines on a SiO_2/Si substrate represented by rotation axis/angle pairs (left: rotation axes of smallest rotation angles; right: two intervals of rotation angle).

large-angle grain boundaries are clearly visible. Other frequently used representations for misorientations are the Σ characterisation of grain boundaries, and the rotation-axis/rotation-angle description (Rodrigues vector).

It is worth noting that the small green grains (i.e. close to <011> oriented grains) and the red grain (i.e. close to <001> oriented grains) in the specimen-normal map of Fig. 6 indicate candidates for thermomechanical hillock growth. As has been shown earlier in a TEM investigation of individual grain orientations (Schwarzer and Gerth, 1993), hillocks deviate from the ordinary 111 fibre texture of aluminium sputter layers. They are formed if there is a strong thermomechanical misfit with the substrate, a diffusion path available along grain boundaries or to triple points, and a sufficient misorientation with the neighbouring grains. The softer grains which significantly deviate from the common 111 fibre axis are preferentially deformed during the heating cycle and thermomechanical stress can be relaxed by material transport from the harder grains. During the cooling cycle, however, diffusion is inhibited due to a lower temperature and the mass transport cannot be reversed. Finally, mass depletion and grain collapse take place at the harder grains, while mass is accumulated during thermal cycling at locations far away from the common 111 fibre orientation.

XII. CONCLUSIONS

Electron diffraction Kikuchi patterns provide the microscopist with a convenient means of obtaining crystallographic information on a subgrain scale. For the study of preferred grain orientations (crystallographic 'texture'), a large number of individual grain orientations have to be known, which makes it necessary to perform the interpretation of diffraction patterns on a computer.

A fully automated system for the acquisition and interpretation of backscatter Kikuchi patterns in a computer-controlled SEM has been presented. The primary beam is digitally scanned (12-bit depth) in a regular grid pattern across the steeply tilted sample surface. The measurement takes less than half a second per image point on a Pentium Pro 200 MHz PC. A data set is, therefore, readily compiled which can be used for the calculation of grain-specific properties or statistical texture functions (ODF, MODF). The digital beam scan for automated crystal-orientation mapping requires the following control operations to be performed by the computer:

- positioning the primary beam spot to the subsequent raster points. Allowance is made for the distortion of the grid pattern due to oblique projection on the specimen surface.

- Control of the objective lens focus to allow for variations in working distance from scan line to scan line, due to the highly tilted surface ("software dynamic focusing").
- Acquisition of the backscatter Kikuchi pattern and contrast enhancement by dividing the digitised actual pattern by a flat image.
- Calculation of the actual pattern centre and the diffraction length ("autocalibration") for each raster point.
- Unattended interpretation of the backscatter Kikuchi pattern and storing the grain orientation.

Crystal orientation maps ('images') are constructed by assigning to each raster point in the image a colour specific to the grain orientation, misorientation or grain boundary character. Colour keys can be stained inverse pole figures, or coloured sections through Euler or Rodrigues orientation spaces. Texture components of interest can be highlighted by distinct colours in the crystal orientation maps in order to reveal texture inhomogeneities. In addition to the determination of misorientations across grain boundaries and the classification of grain boundary character, the normals of grain boundaries can be indexed by a supplementary evaluation of microstructure images.

Acknowledgements—Financial support by the German Research Foundation (DFG-Forschergruppe "Textur und Anisotropie kristalliner Stoffe") is gratefully acknowledged. Dr Frank Springer and Marco Lepper are gratefully acknowledged for the orientation maps in Figs 6 and 7. The author expresses his appreciation to Professor Ray Egerton for carefully reading the manuscript and helpful suggestions.

REFERENCES

Adams, B. L., Wright, S. I. and Kunze, K., 1993. Orientation imaging: the emergence of a new microscopy. *Metallurgical Transactions,* **24A**, 819-831.

Alam, M. N., Blackman, M. and Pashley, D. W., 1954. High-angle Kikuchi patterns. *Proc. Roy. Soc.,* **221,** 224-242.

Bässmann, H. and Besslich, Ph. W., 1993. *Bildverarbeitung Ad Oculos,* 2nd edn. Springer-Verlag, Berlin.

Boersch, H., 1937. Über Bänder bei Elektronenbeugung. *Phys. Z.,* **38**, 1000-1004.

Bollman, W., 1970. C*rystal Defects and Crystalline Interfaces.* Springer-Verlag, Berlin.

Bunge, H.-J., 1982. *Texture Analysis in Materials Science—Mathematical Methods.* Butterworths, London.

Dingley, D. J., 1984. Diffraction from sub-micron areas using electron backscattering in a scanning electron microscope. *Scanning Electron Microscopy,* **2**, 569-575.

Gaukler, K. H. and Schwarzer, R., 1971. Verbessertes Verfahren zur Bestimmung des mittleren inneren Potentials aus Reflexions-Kikuchi-Diagrammen. *Optik,* **33,** 215-229.

Gerth, D. and Schwarzer, R. A., 1993. Graphical representation of grain and hillock orientations in annealed Al-l%Si films. *Textures and Microstructures,* **21**, 177-193.

Gerth, D., Katzer, D. and Schwarzer, R. A., 1994. The influence of local thermomechanical stress on grain growth in thin Al-l%Si layers on SiO_2/Si substrates. *Phys. Stat. Sol. (a),* **146,** 299-316.

von Grote, K. H., 1968/69. Bestimmung des mittleren inneren Potentials aus Kikuchi-Diagrammen von Wolfram-Einkristallen. *Optik,* **28**, 374-388.

Hashimoto, H., Howie, A. and Whelan, M. J., 1962. Anomalous electron absorption effects in metal foils. *Proc. Royal Soc.,* **269A**, 80.

Heise, F., 1952. Ein Zusatzgerät für Elektronenbeugung mit streifendem Einfall. *Optik,* **9**, 139-142.

Helming, K., Rauschenbach, B. and Schwarzer, R.A., 1996. Analysis of crystallographic texture in small sample areas. *Textures and Microstructures,* **26-27**, 111-124.

Hjelen, J., Ørsund, R., Hoel, E., Runde, P., Furu, T. and Nes, E.,1993. EBSP. Progress in technique and applications. *Textures and Microstructures,* **20**, 29-40.

Hough, P. V. C., 1962. A method and means for recognizing complex patterns. US Patent 3,069,654.

ICOTOM-10, 1994. Proc. 10th International Conference on Textures of Materials, Clausthal, 1993, ed. H. J. Bunge. Materials Science Forum.

ICOTOM-11: Proc. 11th International Conference on Textures of Materials, Xi'an China, 1996, eds Z. Liang, L. Zuo and C. Youyi. International Academic Publishers, Beijing. ISBN 7-80003-376-7/ TG.26.

Illingworth, J. and Kittler, J., 1988. A survey of the Hough transform. *Computer Vision, Graphics and Image Processing,* **44,** 87-116.

Ino, Sh., 1977. Some new techniques in reflection high energy electron diffraction (RHEED). Application to surface structure studies. *Jap. J. Appl. Phys.,* **16**, 891-908.

Juul Jensen, D. and Schmidt, N. H., 1991. Local texture measurements by EBSP. New computer procedures. *Textures and Microstructures,* **14-18,** 97-102.

Schmidt, N. H. and Olesen, N. Ø., 1989. Computer-aided determination of crystal-lattice orientation from electron-channeling patterns in the SEM. *Canadian Mineralogist,* **27**, 15-22.

Kikuchi, S., 1928. Diffraction of cathode rays by mica. *Jap. J. Phys.,* **5**, 83-96.

Krieger Lassen, N. C., Juul Jensen, D. and Conradsen, K., 1992. Image processing procedures for analysis of electron backscattering patterns. *Scanning Microscopy,* **6**, 115-121.

Krieger Lassen, N. C. and Bilde-Sørensen, J. B., 1993. Calibration of an electron back-scattering pattern set-up. *J. Microscopy,* **170,** 125-129.

Krieger Lassen, N. C., 1994. Automated determination of crystal orientations from electron backscattering patterns. Ph.D. thesis, Danmarks Tekniske Universitet, Lyngby.

Krieger Lassen, N. C., 1995. Computerized analysis of Kikuchi patterns. Proc. 16th Risø Intern. Symp. on Materials Science, eds. N. Hansen, D. Juul Jensen, Y. L. Liu and B. Ralph. Roskilde, pp. 405-411.

von Laue, M.,1944. Materiewellen und ihre Interferenzen. Akademische Verlagsges. Geest und Portig K. G., Leipzig.

Michael, J. R. and Goehner, R. P., 1993. Crystallographic phase identification in the scanning electron microscope: Backscattered electron Kikuchi patterns imaged with a CCD-based detector. *MSA Bulletin,* **23**, 168-175.

Niedrig, H., 1978. Physical background of electron backscattering. *Scanning,* **1**, 17-34.

Nishikawa, Sh. and Kikuchi, S., 1928. The diffraction of cathode rays by calcite. *Proc. Imp. Acad. Japan,* **4**, 475-477.

Radon, J., 1917. Über die Bestimmung von Funktionen durch ihre Integralwerte längs gewisser Mannigfaltigkeiten. Berichte Sächsische Akademie der Wissenschaften. *Math.-Phys. Klasse, Leipzig,* **69,** 262-267.

Randle, V., 1992. *Microtexture Determination and its Applications.* Inst. Materials, London.

Randle, V., 1993. *Measurement of Grain Boundary Geometry.* IOP Bristol.

Reimer, L., 1979. Electron diffraction methods in TEM, STEM and SEM. *Scanning,* **2**, 3-19.

Reimer, L. and Grün, D., 1986. Zur Aufzeichnung von Elektronen-Rückstreu-Diagammen (EBSP) in einem SEM. *BEDO,* **19,** 105-110.

Reimer, L., Heilers, U. and Saliger, G., 1986. Kikuchi band contrast in diffraction patterns recorded by transmitted and backscattered electrons. *Scanning,* **8**, 101-118.

Riecke, W. D. and Sakaki, Y., 1959. Zur Untersuchung des reziproken Gitters von Einkristallen mit Hilfe von Kikuchi-Diagrammen. *Z. Physik,* **156**, 534-554.

Schmidt, N. H., Bilde-Sørensen, J. B. and Juul Jensen, D., 1991. Band positions used for on-line crystallographic orientation determination from electron back scattering patterns. *Scanning Electron Microscopy,* **5**, 637-643.

Schumann, H., 1979. *Kristallgeometrie.* VEB-Verlag, Leipzig.

Schwarzer, R. and Weiland, H., 1984. On-line computerized evaluation of Kikuchi patterns for the determination of

preferred orientations and orientation correlations. Proc. 7th Intern. Conf. on Textures of Materials (ICOTOM 7), Holland 1984, pp. 839-843.

Schwarzer, R., 1989. Die Aufnahme von Reflexions-Kikuchi-Diagrammen im REM mit einer peltiergekühlten, integrierenden CCD-Videokamera. *BEDO,* **22**, 279-282.

Schwarzer, R. A., 1991. Crystal texture analysis by means of electron diffraction. In *Advances and Applications of Quantitative Texture Analysis,* eds H. J. Bunge and C. Esling, pp. 51-72. DGM-Verlagsgesellschaft, Oberursel and New York.

Schwarzer, R. A., 1993. The determination of local texture by electron diffraction — a tutorial review. *Textures and Microstructures,* **20**, 7-27.

Schwarzer, R. A., 1993b. Crystal texture analysis of ceramics by electron microscopy. *Ceramika,* **42** and *Polski Biuletyn Ceramiczny,* **4**, 59-65.

Schwarzer, R. A. and Gerth, D., 1993. The effect of grain orientation on the relaxation of thermomechanical stress and hillock growth in Al-l%Si conductor layers on silicon substrates. *J. Electronic Materials,* **22**, 607-610.

Schwarzer, R.A., 1994. A CCD camera system for the acquisition of backscatter Kikuchi patterns on an SEM. *Materials Science Forum,* **157-162,** 187-188.

Schwarzer, R.A., 1994. Preparation of high-resistance or sensitive samples for grain orientation measurement with electron microscopes. *Materials Science Forum,* **157-162,** 201-206.

Schwarzer, R.A., Zaefferer, S., 1994. On-line interpretation of SAD channeling patterns. *Materials Science Forum,* **157-162,** 195-200.

Schwarzer, R. A., Zaefferer, S., 1995. Automated measurement of grain orientations and on-line determination of complete deformation systems with a TEM. *Advances in X-Ray Analysis,* **38**, 377-381.

Schwarzer, R. A. and Kunze, K., 1995. The characterization of microtexture by orientation mapping microscopy. *Advances in X-Ray Analysis,* **38**, 547-550.

Schwarzer, R. A., Springer, F. and Zaefferer, S., 1996. Crystal orientation mapping by digital beam scan and automated interpretation of backscatter Kikuchi patterns in the SEM. Proc. l1th Int. Conf. Textures Materials (ICOTOM 11), X'ian, China, pp. 43-52.

Venables, J. A. and Harland, C. J., 1973. Electron back-scattering patterns — a new technique for obtaining crystallographic information in the SEM. *Phil. Mag.,* **27**, 1193-1200.

Venables, J. A. and Bin-Jaya, R., 1977. Accurate microcrystallography using electron back-scattering patterns. *Phil. Mag.,* **35**, 1317-1332.

Watanabe, T., 1983. Observations of plane-matching boundaries by electron channelling patterns. *Phil. Mag. A,* **47**, 141-146.

Weiland, H. and Schwarzer, R., 1985. On-line Auswertung von Kikuchi- und Channelling-Diagrammen. *BEDO,* **18**, 55-60.

Weiland, H. and Schwarzer, R., 1986. On-line texture determination by Kikuchi or channeling patterns. In *Experimental Techniques of Texture Analysis,* ed. H. J. Bunge, pp. 301-313. DGM-Verlagsgesellschaft, Oberursel and New York.

Weiland, H., 1994. Microstructure determination and its application to materials science. *Journal of Metals,* **46**, 37-41.

Wilman, H., 1948. The interpretation and application of electron-diffraction "Kikuchi-line" patterns—Part I: The determination of the crystal unit cell, its orientation and the crystal symmetry. *Proc. Phys. Soc. (London),* **60**, 341-360.

Wright, S. I., Zhao, J. and Adams, B. L., 1991. Automated determination of lattice orientation from electron backscattered Kikuchi diffraction patterns. *Textures and Microstructures,* **13,** 123-131.

Wright, S.I. and Adams, B.L., 1991. Automated lattice orientation determination from electron backscatter Kikuchi diffraction patterns. *Textures and Microstructures,* **14-18,** 273-278.

Zaefferer, S. and Schwarzer, R. A., 1994. Automated measurement of single grain orientations in the TEM. *Z. Metallkunde,* **85**, 585-591.

Zaefferer, S. and Schwarzer, R.A., 1994. On-line determination of complete deformation systems for cubic and hexagonal crystals in the TEM. *Materials Science Forum,* **157-162,** 241-246.

Zaefferer, S. and Schwarzer, R.A., 1994. On-line interpretation of spot and Kikuchi patterns. *Materials Science Forum,* **157-162,** 247-250.

Zaefferer, S., 1996. Entwicklung und Anwendungen eines elektronenmikroskopischen on-line Verfahrens zur Bestimmung von Verformungssystemen in hexagonalen Werkstoffen. Ph.D. thesis, TU Clausthal 1996. Papierflieger Clausthal-Z. ISBN 3-931443-92-2.